# Weak, strong, and uniform quantum simulations

Dong-Sheng Wang*

*Institute for Quantum Science and Technology, Department of Physics and Astronomy, University of Calgary, Alberta, Canada, T2N 1N4*

(Received 5 October 2014; published 23 January 2015)

In this work, we introduce different types of quantum simulations according to different operator topologies on a Hilbert space, namely, uniform, strong, and weak quantum simulations. We show that they have the same computational power that the efficiently solvable problems are in bounded-error quantum polynomial time. For the weak simulation, we formalize a general weak quantum simulation problem and construct an algorithm which is valid for all instances. Also, we analyze the computational power of quantum simulations by proving the query lower bound for simulating a general quantum process.

DOI: 10.1103/PhysRevA.91.012334 PACS number(s): 03.67.Ac, 03.65.Yz

## I. BACKGROUND

In quantum computation, a string of qubits evolves through a sequence of unitary gates and then are measured for the learning of computational results. This process in general includes three stages: preparation, evolution, and measurement. Quantum simulation is motivated to simulate and solve quantum physical problems using quantum computers [1–3] and has been explored so far, corresponding to the three stages, for quantum-state generation [4–7], for approximating unitary and nonunitary evolution [8–13], and for implementing measurement, such as positive operator-valued measure (POVM) [14].

However, there exist diverse notions of simulation and models of quantum simulators, e.g., digital vs analog simulation [3]. The concepts of simulation, emulation, and imitation are closely related and may cause confusion occasionally. In fact, there could be different notions of simulation depending on the simulation subject, object, quality, and other essential factors. In this work, we explore the concept of simulation from both mathematical and physical points of view.

Recently, it was shown that some special kinds of quantum algorithms and quantum circuits can be efficiently simulated by classical computers [15–18]. For the task of simulating quantum algorithms by classical computers, there could be different kinds of simulations, e.g., strong and weak simulations, which prove to be of different computational power [16,17]. This motivates the consideration of different quantum simulations of quantum evolution, and the question whether there exists a computational difference of various quantum simulations.

We consider a quantum simulation problem which could involve all three stages of a quantum process. Different simulation problems would require different solutions (algorithms). As quantum evolution is generally described by operators and operator dynamics, we find that a natural mathematical framework to classify quantum simulations involves the operator topologies on a Hilbert space [19]. There exist three types of commonly used operator topologies: uniform (or norm), strong, and weak operator topologies. Accordingly, we construct three different kinds of quantum simulations, namely, uniform, strong, and weak quantum simulations, and provide proper physical interpretations of them.

The quantum simulation mostly considered so far in the literature is the strong simulation, (e.g., Ref. [2]). In this work, we focus on uniform and weak quantum simulations, which have not been widely explored. Note that our notions of strong and weak quantum simulations are different from the classical simulations in Refs. [16,17].

We first show that the computational powers of these different simulations are the same. It is not possible to simulate a quantum process which cannot be implemented by a BQP circuit efficiently for all kinds of simulations. By a "BQP circuit" we mean a quantum circuit that can efficiently solve problems in bounded-error quantum polynomial time (BQP).

We formalize a weak quantum simulation problem of simulating a quantum process with a prepared initial system state $\rho$, evolution (which could be a unitary operator or completely positive map) $\mathcal{E}$, and measurement result on observable $\hat{O}$ such that the expectation value $\langle \hat{O} \rangle$ on the final state can be approximated within error tolerance $\epsilon$ for all instances $\rho$. An algorithm is constructed to solve this problem with complexity $O(N^2)$ for $N$ as the dimension of the system. The simulation cost is the same as that of a strong simulation algorithm if a strong quantum simulation is considered [20], which is consistent with our observation that all kinds of simulations have the same computational power.

Different from the circuit model, the query model is also widely employed for the study of computational complexity and the design of algorithms. Previously, the query lower bound for the generation of a general pure quantum state is shown to be $\Omega(\sqrt{N})$, following from Grover's searching algorithm [21]. In this work, the lower bound for (all three kinds of) quantum simulation of one general quantum process is shown in the query model. We prove that the query lower bound for quantum simulation is also $\Omega(\sqrt{N})$, instead of $\Omega(N)$ as one might expect, by establishing a connection between the quantum simulation problem and the quantum-state generation problem.

This work contains the following parts. In Sec. II, we introduce the three kinds of quantum simulations based on operator topologies. We show that these simulations are computationally equivalent. In Sec. III, we study the weak quantum simulation problem and construct an algorithm for it. In Sec. IV, we prove the query lower bound for the quantum simulation problem. We conclude in Sec. V.

*dongshwa@ucalgary.ca

 

## II. QUANTUM SIMULATION FRAMEWORKS

We consider a finite-dimensional Hilbert space $\mathscr{H}$ and the set of bounded linear operators $\mathcal{B}(\mathscr{H})$ acting on it. Given a quantum operator, which could be a density operator (state), unitary operator, nonunitary completely positive map (evolution), or Hermitian operator (observable), the task of simulation is to find one approximation of it or its properties within some distance quantified by a properly chosen metric, and the distance could be reduced if the approximate operator could converge to the given operator. Mathematically, the problem of simulation can be characterized by notions from the topology of bounded linear operators on the Hilbert space [19]. There exist different kinds of convergence in different topologies of the set of bounded linear operators on a Hilbert space. Most commonly, there are uniform (also called norm), strong operator, and weak operator topologies.

(1) *Uniform topology:* For a finite-dimensional Hilbert space $\mathscr{H}$, the uniform topology on the set of bounded linear operators $\mathcal{B}(\mathscr{H})$ is the norm convergence; i.e., $\tilde{T}_i \to T$ in norm if $\lim_{i\to\infty} \|\tilde{T}_i - T\| = 0$, for $T, \tilde{T}_i \in \mathcal{B}(\mathscr{H})$.

(2) *Strong operator topology:* For a finite-dimensional Hilbert space $\mathscr{H}$, the strong operator topology on the set of bounded linear operators $\mathcal{B}(\mathscr{H})$ is the pointwise norm convergence; i.e., $\tilde{T}_i \to T$ strongly if $\lim_{i\to\infty} \|(\tilde{T}_i - T)|\psi\rangle\| = 0$, for $T, \tilde{T}_i \in \mathcal{B}(\mathscr{H})$, and $\forall\ |\psi\rangle \in \mathscr{H}$.

(3) *Weak operator topology:* For a finite-dimensional Hilbert space $\mathscr{H}$, the weak operator topology on the set of bounded linear operators $\mathcal{B}(\mathscr{H})$ is the pointwise weak convergence; i.e., $\tilde{T}_i \to T$ weakly if $\lim_{i\to\infty} |\langle\psi|\tilde{T}_i - T|\phi\rangle| = 0$, for $T, \tilde{T}_i \in \mathcal{B}(\mathscr{H})$, and $\forall\ |\psi\rangle, |\phi\rangle \in \mathscr{H}$.

Correspondingly, we introduce three kinds of quantum simulations and discuss examples for these simulations.

*Definition 1: Weak quantum simulation.* Given one quantum operator $T \in \mathcal{B}(\mathscr{H})$ for a finite-dimensional Hilbert space $\mathscr{H}$, the weak quantum simulation is to approximate $T$ by $\tilde{T}$ within distance $\epsilon > 0$ such that $|\langle\psi|\tilde{T} - T|\psi\rangle| \leqslant \epsilon, \forall\ |\psi\rangle \in \mathscr{H}$.

Note that this definition slightly deviates from the weak operator topology in that the expectation value of the operator is involved, which is related to measurement of an observable, instead of the value evaluated with two different states $|\psi\rangle$ and $|\phi\rangle$. Although a "weak value" (the notion "weak" is used in a different sense) could exist when postselection is considered [22], here we limit ourselves to the standard context of quantum computing and standard quantum mechanics.

*Definition 2: Strong quantum simulation.* Given one quantum operator $T \in \mathcal{B}(\mathscr{H})$ for a finite-dimensional Hilbert space $\mathscr{H}$, the strong quantum simulation is to approximate the action of $T$ on state $|\psi\rangle \in \mathscr{H}$ by $\tilde{T}$ within vector 2-norm distance $\epsilon > 0$ for the worst case such that $\|T - \tilde{T}\| := \sup_{|\psi\rangle} \|(T - \tilde{T})|\psi\rangle\| \leqslant \epsilon$.

*Example 1: Strong quantum simulation of unitary operator.* The problem of strong quantum simulation of one unitary operator $U$, e.g., $U = e^{-iHt}$ if it is generated by a time-independent Hamiltonian $H$, is to approximate it by another unitary $\tilde{U}$ satisfying the spectral norm distance condition $\|U - \tilde{U}\| \leqslant \epsilon$. The approximation can be achieved by, e.g., either constructing an approximate Hamiltonian $\tilde{H}$ using easy-to-implement interactions or using a direct approximation $\tilde{U}$ using elementary quantum gates.

*Example 2: Quantum-state generation.* The problem of quantum-state generation is to generate a state $|\psi\rangle$ within distance $\epsilon$ so that $\||\psi\rangle - |\tilde{\psi}\rangle\| \leqslant \epsilon$. Now suppose $|\psi\rangle = U|0\rangle$, and $|\tilde{\psi}\rangle = \tilde{U}|0\rangle$ for some unitary operators $U$ and $\tilde{U}$, and then the accuracy condition becomes $\|U|0\rangle - \tilde{U}|0\rangle\| \leqslant \epsilon$, which can be ensured if we can simulate $U$ by $\tilde{U}$ strongly; i.e., $\|U - \tilde{U}\| \leqslant \epsilon$.

*Definition 3: Uniform quantum simulation.* Given one quantum operator $T \in \mathcal{B}(\mathscr{H})$ for a finite-dimensional Hilbert space $\mathscr{H}$, the uniform quantum simulation is to approximate $T$ by $\tilde{T}$ within distance $\epsilon > 0$ quantified by a certain operator norm.

*Example 3: Uniform quantum simulation of a unitary operator.* For unitary operator $U$, the uniform quantum simulation is to approximate it without referring to its effects on states or observables. As $\|\bullet\| \leqslant \|\bullet\|_{\mathrm{F}} \leqslant \|\bullet\|_1$ (where $\|\bullet\|$ denotes a spectral norm), the norm to be employed can be the trace norm $\|\bullet\|_1$ or the Frobenius norm $\|\bullet\|_{\mathrm{F}}$. The uniform quantum simulation of $U$ is to approximate it by $\tilde{U}$ such that $\|U - \tilde{U}\|_{\mathrm{F}(1)} \leqslant \epsilon$. It is obvious that the uniform simulation is stronger than the strong simulation of one unitary operator.

The different quantum simulations have natural physical interpretations. The scenario for a uniform quantum simulation is that, given an unknown process, one would like to simulate or approximate the process itself after knowing enough information about the process. One closely related, yet not the same, task is the quantum process tomography, for which one needs to construct the process matrix of the process itself. For strong quantum simulation, one has to make sure that the output state from a simulator is close enough to the ideal output state for any input state. This only requires that the simulator has similar effects on all input states. The requirement of weak quantum simulation is merely to ensure that the simulation provides similar observable effects for a given quantum state and observable, without referring to quantum process tomography or state tomography.

The definitions above can be generalized to the case of simulation of linear mappings $\mathcal{E} \in \mathcal{B}(\mathscr{D})$, with $\mathscr{D} \equiv \mathcal{B}(\mathscr{H})$. We focus on quantum channels in which case $\mathscr{D}$ is the set of density operators also forming a Hilbert space. A channel $\mathcal{E}$ is usually represented by the set of Kraus operators $\{K_i\}$ [23]. As well, from channel-state duality [24,25], there exists the Choi-Jamiołkowski isomorphism $\mathcal{J} : \mathscr{D} \to \mathscr{H} \otimes \mathscr{H}$ and equivalently $\mathcal{J} : \mathcal{B}(\mathscr{D}) \to \mathcal{B}(\mathscr{H} \otimes \mathscr{H})$, which maps the operator $\mathcal{E} \in \mathcal{B}(\mathscr{D})$ into a quantum state, termed the Choi state $\mathcal{C} \in \mathcal{B}(\mathscr{H} \otimes \mathscr{H})$.

For weak quantum simulation with respect to channels, since there is no so-called superobservable living in $\mathcal{B}(\mathscr{D})$, we need to consider an observable living in $\mathcal{B}(\mathscr{H})$ instead.

*Weak quantum simulation II.* Given one quantum operator $T \in \mathcal{B}(\mathscr{H})$, the weak quantum simulation is to approximate $T$ by $\tilde{T}$ within the distance $\epsilon > 0$ such that $\mathrm{tr}((T - \tilde{T})\rho) \leqslant \epsilon, \forall\ \rho \in \mathscr{D}$.

*Example 4: Weak quantum simulation of an observable.* Let the operator be one quantum observable $A$. The simulation accuracy condition is $\sup_\rho |\mathrm{tr}(A\rho) - \mathrm{tr}(\tilde{A}\rho)| \leqslant \epsilon$. In detail, $\mathrm{tr}(A\rho) - \mathrm{tr}(\tilde{A}\rho) = \mathrm{tr}(A_t\rho_0) - \mathrm{tr}(\tilde{A}_t\rho_0)$ in the Heisenberg picture, $A_t$ is the evolved observable $\mathcal{E}(A)$ for a certain channel $\mathcal{E}$, and $\rho_0$ is the initial state, while in the Schrödinger picture,

$\mathrm{tr}(A\rho) - \mathrm{tr}(\tilde{A}\rho) = \mathrm{tr}(A\rho_t) - \mathrm{tr}(A\tilde{\rho}_t)$, and the final state is $\rho_t = \mathcal{E}(\rho)$. The weak quantum simulation can be guaranteed by strong quantum simulation or quantum mixed-state generation, since $\|\rho - \tilde{\rho}\|_1 \leqslant \epsilon$ implies $|\mathrm{tr}(A\rho) - \mathrm{tr}(A\tilde{\rho})| \leqslant \epsilon\|A\|$, following from properties of the trace norm.

*Strong quantum simulation II.* Given one quantum operator $\mathcal{E} \in \mathcal{B}(\mathscr{D})$, the strong quantum simulation is to approximate the action of $\mathcal{E}$ on $\rho \in \mathscr{D}$ by $\tilde{\mathcal{E}}$ within the trace distance $\epsilon > 0$, such that the diamond norm distance [26] satisfies $\|\mathcal{E} - \tilde{\mathcal{E}}\|_\diamond \leqslant \epsilon$.

*Example 5: Strong quantum simulation of channels.* For quantum channel simulation, the strong simulation is to simulate the evolution $\mathcal{E}$; e.g., $\mathcal{E} = e^{\mathcal{L}t}$ if it is generated by a time-independent Liouvillian $\mathcal{L}$, by another operator $\tilde{\mathcal{E}}$ satisfying $\|\mathcal{E} - \tilde{\mathcal{E}}\|_\diamond \leqslant \epsilon$, or the induced Schatten 1-norm distance (when no correlation of the system to others is allowed) $\|\mathcal{E} - \tilde{\mathcal{E}}\|_{1\to1} := \sup_\rho \|(\mathcal{E} - \tilde{\mathcal{E}})\rho\|_1 \leqslant \epsilon$. This is a generalization of Example 1.

*Example 6: Quantum mixed-state generation.* The problem is to generate a state $\rho$ within distance $\epsilon$, so that $\|\rho - \tilde{\rho}\|_1 \leqslant \epsilon$. Now suppose $\rho = \mathcal{E}(\rho_0)$, and $\tilde{\rho} = \tilde{\mathcal{E}}(\rho_0)$. The simulation can be ensured if we can simulate $\mathcal{E}$ by $\tilde{\mathcal{E}}$ strongly; i.e., $\|\mathcal{E} - \tilde{\mathcal{E}}\|_\diamond \leqslant \epsilon$. This is a generalization of Example 2.

*Uniform quantum simulation II.* Given one quantum operator $\mathcal{E} \in \mathcal{B}(\mathscr{D})$, the uniform quantum simulation is to approximate $\mathcal{E}$ by $\tilde{\mathcal{E}}$ within the distance $\epsilon > 0$ quantified by a certain operator norm.

*Example 7: Uniform quantum simulation of channels.* As we have seen from the channel-state duality, a channel can be represented by a single matrix. As the result, we need to consider uniform simulation in the Choi state representation. The norm we employ is the trace norm on the Choi state. Then, the norm simulation of a quantum channel represented by Choi state $\mathcal{C}$ is to approximate $\mathcal{C}$ by $\tilde{\mathcal{C}}$ such that $\|\mathcal{C} - \tilde{\mathcal{C}}\|_1 \leqslant \epsilon$. Since $N\|\mathcal{C} - \tilde{\mathcal{C}}\|_1 \geqslant \|\mathcal{E} - \tilde{\mathcal{E}}\|_\diamond \geqslant \|\mathcal{E} - \tilde{\mathcal{E}}\|_{1\to1}$ [27], for system dimension $N$, the uniform simulation is stronger than the strong simulation of channels. This is a generalization of Example 3.

In the above we have defined three types of quantum simulations, and it is evident that there exists an "order" in their simulation powers. For instance, for one problem an efficient strong quantum simulation algorithm implies there also exists an efficient weak quantum simulation algorithm. For these different simulations, one of the most basic questions is whether their "efficient simulation domains" are the same. We define the efficient simulation domain as the set of problems which can be efficiently solved by a certain simulation method. The following theorem basically manifests that, although there could be different simulations and simulation algorithms, their simulation powers are constrained by the computational power of quantum computing.

*Theorem 1.* The efficient simulation domains of uniform, strong, and weak quantum simulations are the same, which is BQP.

*Proof.* To prove the claim, we need to show that the smallest possible domain, which is that for uniform simulation, and the largest possible domain, which is that for weak simulation, are both BQP. For uniform simulation, based on channel-state duality, the efficient state generation of a Choi state ensures the efficiency of uniform simulation. For weak simulation, it is not possible to simulate any process beyond BQP efficiently, since weak simulation requires quantum-state generation for a certain state, which only serves to produce approximate observable effects. A state which cannot be prepared by a BQP circuit cannot be efficiently generated. The theorem then follows. ■

## III. WEAK QUANTUM SIMULATION

In this section, we define the weak quantum simulation problem and provide a concise algorithm for solving it, which contains a classical preprocessing part and a quantum circuit to realize the algorithm. It turns out the circuit complexity is in general the same as that for a strong simulation algorithm. We focus on the general case instead of efficient simulation for special cases.

*Weak quantum simulation problem.* For one $N$-dimensional quantum system prepared in state $\rho$, and measured by POVM $\mathcal{M} = \{M_i; i = 0,1,\ldots,m \leqslant N^2\}$ for an observable $\hat{O}$ after an evolution $\mathcal{E}$, which is a quantum channel, construct an efficient quantum circuit, implemented using a universal set of gates, which can approximate the expectation value $\langle\hat{O}\rangle$ on the final state within the error tolerance $\epsilon$ for all instances $\rho$.

Before our analysis, it is better to note the differences from strong simulation. If strong quantum simulation is considered, one needs to simulate the evolution $\mathcal{E}$ itself, whereas for weak quantum simulation one does not necessarily have to do this. Also, the POVM $\mathcal{M}$ is not required to be simulated; instead, one only needs to approximate the expectation value $\langle\hat{O}\rangle$ for all instances.

Furthermore, for weak quantum simulation there could also be different algorithms. The problem merely requires the approximation of $\langle\hat{O}\rangle$ without specifying how to approximate it. A notable example is the simulation method based on the matrix product state [28,29], which employs an open-system dynamics to approximate the dynamical observable of a many-body system based on a duality mapping. One can use a quantum circuit to realize the open-system dynamics, and then the simulation of the many-body system is in fact a weak quantum simulation, and the analysis of the duality relation is the classical part of this simulation method. In the following we present an algorithm which contains a classical analysis of the probability distribution $\{p_i\}$ [in Eq. (2)] and a quantum circuit for the weak simulation.

With the POVM $\{M_i\}$, an observable $\hat{O}$ can be expressed as

$$\hat{O} = \sum_{i=1}^{m} o_i M_i, \tag{1}$$

for

$$p_i = \mathrm{tr}(\rho_f M_i), \tag{2}$$

$$\langle\hat{O}\rangle = \mathrm{tr}(\rho_f \hat{O}) = \sum_{i=1}^{m} o_i p_i, \tag{3}$$

with final state $\rho_f = \mathcal{E}(\rho)$. Given the set $\{M_i\}$ and $\hat{O}$, we can obtain $o_i$ explicitly. Then the problem to approximate $\langle\hat{O}\rangle$ is reduced to the approximation of the probability distribution $\{p_i\}$.

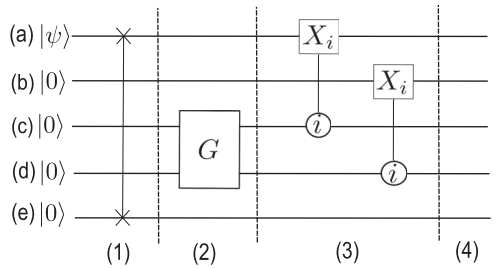


FIG. 1. The circuit for the replacement channel $\mathcal{R}$. The leftmost gate with two crosses represents a qudit swap gate. A circle with $i$ in it means an $i$ control, and $X_i$ is the Pauli $X$ operator between states $|0\rangle$ and $|i\rangle$. The controlled $X_i$ represents a qudit controlled-NOT (CNOT) gate, and here there are a sequence of such CNOT gates for all $i$. The bottom three ancillas are traced out finally.

The next step in our method is to construct a quantum circuit, which can map any state $\rho$ onto a well-defined state $\sigma$, projective measurement on which yields the (approximate) probability distribution $\{p_i\}$. Without loss of generality, we assume $m = N^2$ and denote $N \equiv d$; i.e., the system is a qudit. One easily finds that the state $\sigma$ can be chosen as

$$\sigma = \mathrm{diag}(p_0, p_1, \ldots, p_{d^2-1}). \tag{4}$$

We employ the *replacement channel* $\mathcal{R}$ to map any state $\rho$ onto $\sigma$:

$$\mathcal{R}(\rho) = \sigma = \sum_{i,j} K_{ij} \rho K_{ij}^{\dagger}, \tag{5}$$

with Kraus operators

$$K_{ij} = \sqrt{p_i}|i\rangle\langle j|, \tag{6}$$

for $0 \leqslant i \leqslant d^2 - 1$, $0 \leqslant j \leqslant d - 1$.

Note that the state $\sigma$ has higher dimension than the input state $\rho$, which implies that a qudit ancilla is required. Also, there are $d^3$ Kraus operators, so another three qudit ancillas are required for the implementation of this channel. The index $i$ in $K_{ij}$ can be split into two indices, $i_1$ and $i_2$ with $0 \leqslant i_1, i_2 \leqslant d - 1$, and $p_i \equiv p_{i_1 i_2}$.

The quantum circuit to implement the channel $\mathcal{R}$ is shown in Fig. 1. We use the $d$-ary representation in the circuit diagram, so each wire represents a qudit. There are five registers (from top to bottom): Fig. 1(a), the system; Fig. 1(b), the ancilla which is a part of the output system; and Figs. 1(c)–1(e), the bottom three ancillas to implement the projections.

The gate $G$ is defined as

$$G|0\rangle|0\rangle = \sum_i \sqrt{p_i}|i\rangle = \sum_{i_1,i_2} \sqrt{p_{i_1 i_2}}|i_1\rangle|i_2\rangle \tag{7}$$

and can be realized by an $O(d^2)$ sequence of rotations $\{G_{i,i+1}\}$ which only act on two basis states

$$G = \prod_{i=d^2-1}^{0} G_{i,i+1}, \quad G_{i,i+1}|i\rangle = \cos\theta_i|i\rangle + \sin\theta_i|i+1\rangle, \tag{8}$$

containing $d^2$ parameters $0 \leqslant \theta_i \leqslant 2\pi$, which can be obtained from $p_i$ based on the following concise relations:

$$p_i = \sum_{S_i \subseteq S} \prod_{n \in S_i} \sin\theta_n \prod_{m \notin S_i} \cos\theta_m, \tag{9}$$

where $S$ denotes the set $\{0, 1, \ldots, d^2 - 1\}$, $S_i$ denotes the set $\{\alpha_1, \ldots, \alpha_i\}$, and $\alpha_1 \neq \alpha_2 \neq \cdots \neq \alpha_i \in S$.

Next we show the action of the quantum circuit. For input state $|\psi\rangle|0\rangle|0\rangle|0\rangle|0\rangle$ with system state $|\psi\rangle = \sum_{j=0}^{d-1} c_j|j\rangle$, the quantum circuit proceeds as follows:

(1) The swap gate leads to $|0\rangle|0\rangle|0\rangle|0\rangle|\psi\rangle$.

(2) The gate $G$ leads to $|0\rangle|0\rangle(\sum_{i_1,i_2} \sqrt{p_{i_1 i_2}}|i_1\rangle|i_2\rangle)|\psi\rangle$.

(3) The two sequences of CNOT gates yield the state $(\sum_{i_1,i_2} \sqrt{p_{i_1 i_2}}|i_1\rangle|i_2\rangle|i_1\rangle|i_2\rangle)|\psi\rangle$.

(4) The projector $P_{ij} = |i_1, i_2, j\rangle\langle i_1, i_2, j|$ on the bottom three ancillas leads to the state $\sqrt{p_{i_1 i_2}} c_j|i_1\rangle|i_2\rangle$ which is equivalent to the action $K_{ij}|\psi\rangle$.

We see that the projective measurement

$$\mathcal{P} = \{P_{ij}; P_{ij} = |i,j\rangle\langle i,j|, \quad 0 \leqslant i \leqslant d^2 - 1, \\ 0 \leqslant j \leqslant d - 1\} \tag{10}$$

realizes the Kraus operators $\{K_{ij}\}$ and leads to the probability distribution $\{p_i c_j^2\}$. The distribution $\{p_i\}$ is obtained by combining $p_i c_j^2$ for all $j$s since $\sum_j p_i c_j^2 = p_i$.

In order to ensure the simulation accuracy, a weak quantum simulation accuracy condition is defined as

$$\sup_{\rho} |\langle \hat{O} \rangle - \langle \tilde{\hat{O}} \rangle| \leqslant \epsilon. \tag{11}$$

In order to satisfy this, we require

$$\|\mathcal{R} - \tilde{\mathcal{R}}\|_{\diamond} \leqslant \epsilon \|\hat{O}\|/2, \tag{12}$$

which implies

$$\sup_{\rho} D_t(\sigma, \tilde{\sigma}) \leqslant \epsilon \|\hat{O}\|/2, \tag{13}$$

and then the weak simulation accuracy condition in Eq. (11) is satisfied. Condition (12) can be ensured if the whole circuit unitary operator $U$ can be approximated by $\tilde{U}$ such that $\|U - \tilde{U}\| \leqslant \epsilon\|\hat{O}\|/4$, since $\|\mathcal{R} - \tilde{\mathcal{R}}\|_{\diamond} \leqslant 2\|U - \tilde{U}\|$ [10]. The $\|\hat{O}\|$ is the spectral norm of observable $\hat{O}$.

Next we analyze the complexity of the circuit. The $O(d^2)$ sequence of gates $G_{i,i+1}$ can be realized by a sequence of single-qubit gates and CNOT gates in the same order. There are $O(d^2)$ controlled-$X_i$ gates, and the swap gate can be realized by $O(d)$ CNOT gates. Employing Solovay-Kitaev-type algorithms for single-qubit gate compiling [30–32], the complexity of the circuit becomes $O(d^2 \log_2 \frac{d^2}{\epsilon})$.

For strong quantum simulation of one unitary evolution $U \in \mathrm{SU}(d)$ or quantum channel $\mathcal{E}$, the circuit complexity is $O(d^2 \log_2 \frac{d^2}{\epsilon})$ [33]. By comparison, one finds the complexity is the same for weak and strong quantum simulations. This is reasonable since a POVM with $d^2$ elements is informationally complete so that the final state can be fully reproduced. If there are fewer POVM elements, the weak simulation cost could be smaller than that for strong simulation. For instance, for a POVM with $d$ elements, the circuit complexity reduces to $O(d \log_2 \frac{d}{\epsilon})$.

## IV. QUERY LOWER BOUND FOR QUANTUM SIMULATION

In this section, we study the query lower bound for quantum simulation. The quantum query model for unitary operation simulation has been investigated [34–36], yet the query lower bound is unknown. Here our method to prove the lower bound is to consider the uniform quantum simulation.

Instead of designing a quantum circuit based on channel parameters, in the query model the parameters are provided in a black box, i.e., *oracle*, which can only be queried by an oracle call to extract limited information of the channel each time. The total number of queries to this oracle and others to be used are counted as the query complexity.

*Uniform quantum simulation problem in the query model.* For a quantum channel $\mathcal{E} \in \mathcal{B}(\mathscr{D})$ acting on an $N$-dimensional system, represented by the set of Kraus operators $\{K_\alpha\}, \alpha = 0, \ldots, N^2-1$, $K_\alpha = \sum_{i,j=0}^{N-1} k_{ij}^{(\alpha)} |i\rangle\langle j|$, there exists an oracle call $O_\alpha$ such that $O_\alpha |i\rangle|j\rangle|\alpha\rangle|0\rangle = |i\rangle|j\rangle|\alpha\rangle|k_{ij}^{(\alpha)}\rangle$. The problem is to simulate $\mathcal{E}$ within error tolerance $\epsilon$ and prove the query lower bound.

Instead of the set of Kraus operators, the channel $\mathcal{E}$ can be equivalently represented by the normalized Choi state $\mathcal{C}$ which takes the form $\mathcal{C} = \mathcal{E} \otimes \mathbb{1}(\omega)$, with $\omega = \frac{1}{\sqrt{N}} \sum_{i=0}^{N-1} |i,i\rangle$. Precisely, the Choi state is

$$\mathcal{C} = \frac{1}{N} \sum_{\alpha=0}^{N^2-1} \sum_{ijkl}^{N-1} k_{ij}^{(\alpha)} k_{kl}^{(\alpha)*} (|i\rangle\langle k|) \otimes (|j\rangle\langle l|). \tag{14}$$

We introduce the uniform simulation accuracy condition, which takes the form

$$\|\mathcal{C} - \tilde{\mathcal{C}}\|_1 \leqslant \frac{\epsilon}{N}. \tag{15}$$

Since $N\|\mathcal{C} - \tilde{\mathcal{C}}\|_1 \geqslant \|\mathcal{E} - \tilde{\mathcal{E}}\|_\diamond \geqslant \|\mathcal{E} - \tilde{\mathcal{E}}\|_{1\to 1}$ [27], the condition above implies the strong and weak simulations of the channel.

The norm $\| \bullet \|_1$ is twice the trace distance, which has the operational meaning of distinguishing two quantum states. That is to say, the successful generation of the Choi state implies the channel can be simulated in the uniform simulation. Following from this, we convert the quantum simulation problem to a quantum-state generation problem; i.e., we consider how to generate a Choi state by a quantum circuit.

A circuit for generating a Choi state is shown in Fig. 2. There are four registers: the controller [Fig. 2(a)], the system [Fig. 2(b)], and two ancillas [Figs. 2(c) and 2(d)]. First, we consider pure quantum-state generation, which is implemented when the controller [Fig. 2(a)] is omitted.

We consider how to generate the dual state of a unitary operator. A unitary operator can be viewed as a channel with only one Kraus operator which is unitary. For unitary operator $U \in \mathrm{SU}(N)$, and $U = \sum_{i,j=0}^{N-1} u_{ij} |i\rangle\langle j|$, its dual Choi state is $|\psi_U\rangle = \frac{1}{\sqrt{N}} \sum_{i,j=0}^{N-1} u_{ij} |i,j\rangle$. The oracle in the circuit does not depend on $\alpha$ in this case. The oracle $O$ works as $O|i\rangle|j\rangle|0\rangle = |i\rangle|j\rangle|u_{ij}\rangle$. Note that the ancilla is not a single qubit. The algorithm follows from Grover's method [21]. The algorithm proceeds as follows:

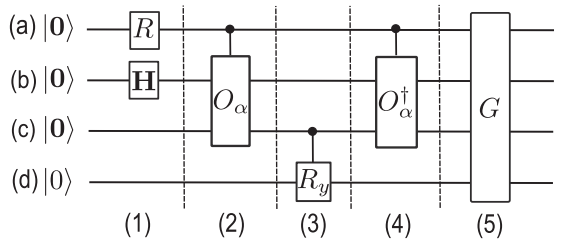


FIG. 2. The circuit for the generation of a mixed state $\rho$. State $|\mathbf{0}\rangle$ in bold represents a qubit string of $|0\rangle$. $R$ is a multiqubit gate to generate superposition depending on the form of the mixed state. **H** is the Walsh-Hadamard gate. $R_y$ is the single-qubit rotation about the $y$ axis. $O_\alpha$ and its Hermitian conjugate are queries. $G$ represents the generalized Grover searching algorithm [37–39]. The controller (a) is traced out at the end. The generation of a pure state is achieved when the controller is omitted, so the query complexities for generation of pure and mixed states are the same.

(1) The Walsh-Hadamard gate **H** leads to the state $\frac{1}{\sqrt{N}} \sum_{i,j=0}^{N-1} |i,j\rangle|\mathbf{0}\rangle|0\rangle$.

(2) From the oracle call we get the state $\frac{1}{\sqrt{N}} \sum_{i,j=0}^{N-1} |i,j\rangle|u_{ij}\rangle|0\rangle$.

(3) The controlled rotation of the $R_y$ gate yields the state $\frac{1}{\sqrt{N}} \sum_{i,j=0}^{N-1} |i,j\rangle|u_{ij}\rangle(u_{ij}|0\rangle + \sqrt{1-u_{ij}^2}|1\rangle)$.

(4) From the inverse oracle call we get the state $\frac{1}{\sqrt{N}} \sum_{i,j=0}^{N-1} |i,j\rangle|0\rangle(u_{ij}|0\rangle + \sqrt{1-u_{ij}^2}|1\rangle)$.

(5) We use Grover's searching algorithm or, generally, amplitude amplification $G$ to convert the second ancilla to $|0\rangle$, which needs the Grover oracle call $O(\sqrt{N})$.

(6) Tracing out the two ancillas [Figs. 2(c) and 2(d)], we get state $|\psi_U\rangle$.

It is known that pure quantum-state generation can be realized by a search algorithm with $O(\sqrt{N})$ queries along with failure probability $O(1/N)$, which could be further reduced to zero with generalized search algorithms [37–39].

For the generation of a mixed Choi state, we first observe that the Choi state takes the form $\mathcal{C} \equiv \sum_{\alpha=0}^{N^2-1} p_\alpha |\psi_\alpha\rangle\langle\psi_\alpha|$, with $|\psi_\alpha\rangle = K_\alpha \otimes \mathbb{1}(\omega) = \frac{1}{\sqrt{N}} \sum_{i,j=0}^{N-1} k_{ij}^{(\alpha)} |i,j\rangle$, and $p_\alpha = \mathrm{tr}[K_\alpha^\dagger K_\alpha \otimes \mathbb{1}(\omega)]$, with $\sum_{\alpha=0}^{N^2-1} p_\alpha = 1$. Although state $|\psi_\alpha\rangle$ is not normalized, the algorithm above for generation of a pure state still applies. The algorithm for generating a Choi state proceeds as follows:

(1) On input state $|\mathbf{0},\mathbf{0},\mathbf{0},0\rangle$, the gate $R$ generates state $\sum_{\alpha=0}^{N^2-1} \sqrt{p_\alpha}|\alpha\rangle|\mathbf{0},\mathbf{0},0\rangle$. Note the state $|\alpha\rangle$ is a computational basis state. After the Walsh-Hadamard gate **H**, the state becomes $\frac{1}{\sqrt{N}} \sum_{\alpha=0}^{N^2-1} \sum_{i,j=0}^{N-1} \sqrt{p_\alpha}|\alpha\rangle|i,j\rangle|\mathbf{0},0\rangle$.

(2) From the controlled oracle call we get the state $\frac{1}{\sqrt{N}} \sum_{\alpha=0}^{N^2-1} \sum_{i,j=0}^{N-1} \sqrt{p_\alpha}|\alpha\rangle|i,j\rangle|k_{ij}^{(\alpha)}\rangle|0\rangle$.

(3) The controlled rotation of the $R_y$ gate yields $\frac{1}{\sqrt{N}} \sum_{\alpha=0}^{N^2-1} \sum_{i,j=0}^{N-1} \sqrt{p_\alpha}|\alpha\rangle|i,j\rangle|k_{ij}^{(\alpha)}\rangle(k_{ij}^{(\alpha)}|0\rangle + \sqrt{1-|k_{ij}^{(\alpha)}|^2}|1\rangle)$.

(4) From the inverse oracle call we get the state $\frac{1}{\sqrt{N}} \sum_{\alpha=0}^{N^2-1} \sum_{i,j=0}^{N-1} \sqrt{p_\alpha}|\alpha\rangle|i,j\rangle|\mathbf{0}\rangle(k_{ij}^{(\alpha)}|0\rangle + \sqrt{1-|k_{ij}^{(\alpha)}|^2}|1\rangle)$.

(5) We use amplitude amplification $G$ to convert the second ancilla to $|0\rangle$, which needs the Grover oracle call $O(\sqrt{N})$.

(6) Tracing out the controller [Figs. 2(a)] and the two ancillas [Figs. 2(c) and 2(d)], we obtain the Choi state.

As the uniform, strong, and weak quantum simulations are computationally equivalent, the query lower bound is the same for all of them. This can be explained by showing that a weak quantum simulation algorithm in the query model can be employed to generate the Choi state of a channel. From quantum process tomography, the expectation values of a set of observables, denoted as $\{\langle\hat{O}_i\rangle\}$, need to be measured. Suppose the query lower bound is $\Omega(\sqrt{N})$ for approximating each $\langle\hat{O}_i\rangle$; then the total query lower bound is still $\Omega(\sqrt{N})$ for process tomography since the approximations for each $\langle\hat{O}_i\rangle$ are in parallel and the lower bounds do not add up together. As a result, we can state the query lower bound regardless of the type of simulations.

As the search algorithm is optimal [40], the following theorem is proved based on the quantum-state generation algorithm above.

*Theorem 2.* The quantum query lower bound to simulate a quantum channel $\mathcal{E}$ acting on an $N$-dimensional system is $\Omega(\sqrt{N})$.

The result shows that the query lower bounds for generating a pure state and a mixed state with the same dimension are the same, and the query lower bounds for simulation of a unitary operator and a quantum channel acting on the same dimensional system are also the same.

*Simple quantum algorithm achieving the query lower bound* Here we provide a quantum algorithm which achieves the query lower bound for strong quantum simulation. The algorithm is a "one-shot" algorithm; that is, it generates the corresponding final state given one initial state within error tolerance for each instance. If we could prepare the initial state and final state successfully, then we say the simulation is successful.

First we consider the strong simulation of a unitary operator. Given $U$ acting on $N$-dimensional $\mathscr{H}$, suppose $U|\lambda_i\rangle = e^{-i\theta_i}|\lambda_i\rangle$, with eigenstate $|\lambda_i\rangle$ and eigenvalue $e^{-i\theta_i}$. Any pure state can be expressed in the form $|\psi\rangle = \sum_{i=0}^{N-1}\psi_i|\lambda_i\rangle$, and the evolution generates the final state $|\psi_f\rangle = \sum_{i=0}^{N-1}\psi_i e^{-i\theta_i}|\lambda_i\rangle$, with each coefficient $\psi_i$ accumulating a phase $e^{-i\theta_i}$. We introduce a unitary operator oracle $O_U|i\rangle|0\rangle = |i\rangle|e^{-i\theta_i}\rangle$, which actually performs phase estimation [41]. Combined with the state oracle $O_\psi|i\rangle|0\rangle = |i\rangle|\psi_i\rangle$, we introduce the oracle $O|i\rangle|0\rangle|0\rangle = |i\rangle|\psi_i\rangle|e^{-i\theta_i}\rangle$. With the circuit for quantum-state generation in Fig. 2, it is easy to see that the initial state $|\psi\rangle$ is generated with two calls to $O_\psi$ and $O(\sqrt{N})$ calls to the oracle in the Grover algorithm, and the final state $|\psi_f\rangle$ is generated with two calls to $O$ and $O(\sqrt{N})$ calls to the oracle in the Grover algorithm. The mixed-state case can be reduced to the pure-state case by expanding a density operator as a mixture of pure states.

Next we consider the strong simulation of a quantum channel. Using results on a strong simulation of a quantum channel based on the convex combination of extreme channels, it is known that a quantum channel acting on an $N$-dimensional system can be simulated by convex combination of $N$ extreme quantum circuits, each having a well-defined structure with one initial and one final unitary operator acting on the system [33]. For the query model, we use oracle calls for the initial and final unitary operators, while the rest of the circuit keeps the same gate operations. The algorithm is the combination of the one for the unitary operator above and the extreme channel circuit. In this way, we can simulate a quantum channel in the query model with the same query complexity as a unitary operator.

## V. CONCLUSION AND DISCUSSION

In this work, we have introduced three types of simulations according to operator topologies on a Hilbert space. We showed that the uniform, strong, and weak quantum simulations have the same computational powers, that their efficient simulation domains are all BQP, and, as well, the query lower bound in the query model for them is the same. Note that the three types of different simulations not only apply to quantum simulation, which simulates some objects employing quantum computers, but also can be easily adapted for other forms of simulations, such as simulation on classical standard computers.

We proposed a weak quantum simulation problem, which focuses on the simulation of an observable quantity instead of only evolutions as usually considered in the strong quantum simulation. The recent work on quantum algorithm computing correlation functions [42] can be considered a type of weak quantum simulation. Also, the weak simulation method has a close connection with the numerical simulation methods employed in the literature, particularly in computational physics. For instance, based on the duality between the partition functions of a $D$ spatial dimensional quantum system and a $(D+1)$-dimensional classical system, the method of simulating a quantum system by a classical one is weak simulation [43].

Back to one of the motivations of this work, which is the classical simulation of quantum computation, there are some open problems at this stage. For instance, Refs. [16,17] found that there exist quantum algorithms that can be efficiently weakly simulated yet not strongly simulated by classical computers. Here the "weak classical simulation" is to sample the quantum computational result, and the "strong classical simulation" is to evaluate the quantum computational result. By rough comparison, the strong classical simulation corresponds to our weak simulation method, as both evaluate observable quantities. It would be interesting if a quantum sampling simulation method (relating to operator topology) can also be defined.

## ACKNOWLEDGMENTS

The author acknowledges USARO, AITF and NSERC for financial support during the period of this work. The author thanks B. C. Sanders, D. W. Berry, P. Høyer, and I. Dhand for discussions at the early stage of this work.

[1] R. P. Feynman, Int. J. Theor. Phys. **21**, 467 (1982).
[2] S. Lloyd, Science **273**, 1073 (1996).
[3] I. M. Georgescu, S. Ashhab, and F. Nori, Rev. Mod. Phys. **86**, 153 (2014).

[4] A. Aspuru-Guzik, A. D. Dutoi, P. J. Love, and M. Head-Gordon, Science **309**, 1704 (2005).
[5] J. Emerson, Y. S. Weinstein, M. Saraceno, S. Lloyd, and D. G. Cory, Science **302**, 2098 (2003).
[6] W. Bruzda, V. Cappellini, H.-J. Sommers, and K. Życzkowski, Phys. Lett. A **373**, 320 (2009).
[7] Y. S. Weinstein, Phys. Rev. A **88**, 062303 (2013).
[8] N. Wiebe, D. W. Berry, P. Høyer, and B. C. Sanders, J. Phys. A: Math. Theor. **44**, 445308 (2011).
[9] S. Raeisi, N. Wiebe, and B. C. Sanders, New J. Phys. **14**, 103017 (2012).
[10] D.-S. Wang, D. W. Berry, M. C. de Oliveira, and B. C. Sanders, Phys. Rev. Lett. **111**, 130504 (2013).
[11] M. Kliesch, T. Barthel, C. Gogolin, M. Kastoryano, and J. Eisert, Phys. Rev. Lett. **107**, 120501 (2011).
[12] K. A. G. Fisher, R. Prevedel, R. Kaltenbaek, and K. J. Resch, New J. Phys. **14**, 033016 (2012).
[13] P. Schindler, M. Müller, D. Nigg, J. T. Barreiro, E. A. Martinez, M. Hennrich, T. Monz, S. Diehl, P. Zoller, and R. Blatt, Nat. Phys. **9**, 361 (2013).
[14] G. Sents, B. Gendra, S. D. Bartlett, and A. C. Doherty, J. Phys. A: Math. Theor. **46**, 375302 (2013).
[15] D. E. Browne, New J. Phys. **9**, 146 (2007).
[16] M. J. Bremner, R. Jozsa, and D. J. Shepherd, Proc. R. Soc. A **467**, 459 (2011).
[17] M. Van den Nest, Quantum Inf. Comput. **11**, 784 (2011).
[18] M. Van den Nest, Quantum Inf. Comput. **10**, 0258 (2010).
[19] B. Blackadar, *Operator Algebras* (Springer-Verlag, Berlin, 2006).
[20] A. Barenco, C. H. Bennett, R. Cleve, D. P. DiVincenzo, N. Margolus, P. Shor, T. Sleator, J. A. Smolin, and H. Weinfurter, Phys. Rev. A **52**, 3457 (1995).
[21] L. K. Grover, Phys. Rev. Lett. **85**, 1334 (2000).
[22] Y. Aharonov, D. Z. Albert, and L. Vaidman, Phys. Rev. Lett. **60**, 1351 (1988).
[23] M. A. Nielsen and I. L. Chuang, *Quantum Computation and Quantum Information* (Cambridge University Press, Cambridge, UK, 2000).
[24] A. Jamiołkowski, Rep. Math. Phys. **3**, 275 (1972).
[25] M.-D. Choi, Linear Algebra Appl. **10**, 285 (1975).
[26] A. Kitaev, A. H. Shen, and M. N. Vyalyi, *Classical and Quantum Computation*, Graduate Studies in Mathematics, Vol. 47 (American Mathematical Society, Providence, RI, 2002).
[27] B. Rosgen and J. Watrous, in *Proceedings of the 20th Annual Conference on Computational Complexity* (IEEE, Piscataway, NJ, 2005), pp. 344–354.
[28] F. Verstraete and J. I. Cirac, Phys. Rev. Lett. **104**, 190405 (2010).
[29] S. Barrett, K. Hammerer, S. Harrison, T. E. Northup, and T. J. Osborne, Phys. Rev. Lett. **110**, 090501 (2013).
[30] C. M. Dawson and M. A. Nielsen, Quantum Inf. Comput. **6**, 81 (2006).
[31] V. Kliuchnikov, D. Maslov, and M. Mosca, Phys. Rev. Lett. **110**, 190502 (2013).
[32] V. Kliuchnikov, arXiv:1306.3200.
[33] D.-S. Wang and B. C. Sanders, arXiv:1407.7251.
[34] S. P. Jordan and P. Wocjan, Phys. Rev. A **80**, 062301 (2009).
[35] D. W. Berry and A. M. Childs, Quantum Inf. Comput. **12**, 29 (2012).
[36] R. Cleve, G. Daniel, M. Mosca, R. D. Somma, and D. Yonge-Mallo, in *Proceedings of the 41st Annual ACM Symposium on Theory of Computing* (ACM, New York, 2009), pp. 409–416.
[37] G. Brassard, P. Høyer, M. Mosca, and A. Tapp, arXiv:quant-ph/0005055.
[38] P. Høyer, Phys. Rev. A **62**, 052304 (2000).
[39] G. L. Long, Phys. Rev. A **64**, 022307 (2001).
[40] C. H. Bennett, E. Bernstein, G. Brassard, and U. Vazirani, SIAM J. Comput. **26**, 1510 (1997).
[41] A. Yu. Kitaev, arXiv:quant-ph/9511026.
[42] J. S. Pedernales, R. Di Candia, I. L. Egusquiza, J. Casanova, and E. Solano, Phys. Rev. Lett. **113**, 020505 (2014).
[43] M. Suzuki, Prog. Theor. Phys. **56**, 1454 (1976).